Korean J. Chem. Eng., **31**(11), 2081-2087 (2014)
DOI: 10.1007/s11814-014-0157-5

pISSN: 0256-1115
eISSN: 1975-7220

Effect of nafion membrane thickness on performance of vanadium redox flow battery

Sanghyun Jeong*, Lae-Hyun Kim, Yongchai Kwon*,†, and Sunhoe Kim***,†**

*Graduate School of Energy and Environment, Seoul National University of Science and Technology, 232, Gongneung-ro, Nowon-gu, Seoul 139-743, Korea
**Department of Chemical and Biomolecular Engineering, Seoul National University of Science and Technology, 232, Gongneung-ro, Nowon-gu, Seoul 139-743, Korea
***Department of New Energy and Resource Engineering, Sangji University, Sangjidae-gil, Wonju-si, Gangwon-do 220-702, Korea
(*Received 15 April 2014 • accepted 2 June 2014*)

Abstract−The performance of vanadium redox ow batteries (VRFBs) using different membrane thicknesses was evaluated and compared. The associated experiments were conducted with Nafion® 117 and 212 membranes that have 175 and 50 μm of thickness, respectively. The charge efficiency (CE) and energy efficiency (EE) of VRFB using Nafion® 117 were higher than those of VRFB using Nafion® 212, while power efficiency was vice versa. In terms of amounts of charge and discharge that are measured in different charging current densities, the amounts in VRFB using Nafion® 212 are more than that in VRFB using Nafion® 117. To further characterize the effect of membrane thickness on VRFB performance, electrochemical impedance spectroscopy (EIS) and UV-*vis.* spectrophotometer (UV-vis) were used. In EIS measurements, VRFB using Nafion® 117 was more stable than that using Nafion® 212, while in UV-vis measurements, vanadium crossover rate of VRFB usingNafion® 212 (0.0125 M/hr) was higher than that of VRFB using Nafion® 117 (0.0054 M/hr). These results are attributed to high crossover rate of vanadium ion in VRFB using Nafion® 212. With these results, vanadium crossover plays more dominant role than electrochemical reaction resistance in deciding performance of VRFB in condition of different membranes.

Keywords: Vanadium Redox Flow Battery, Proton Exchange Membrane, Energy Storage System, Electrical Conductivity, Electrochemical Impedance, Membrane Thickness

INTRODUCTION

Conventional renewable energies like solar cell and wind power are attractive energy sources due to their eco-friendly features. However, basic drawbacks of renewable energies such as random and intermittent power production have prevented wider utilization and commercialization of the renewable energies. To alleviate those problems, building up the appropriate energy storage system (ESS) is highly recommended [1]. To date, there have been many types of ESSs considered. Among them, the VRFB has been paid attention as an attractive ESS in large scale manufacturing because of its fast response to energy demand change, tolerance to deep discharge without fatal damage, long life cycle and easy thermal management [2-6].

A flow battery is an energy storage device in which the electrolytes are stored in two tanks and circulated through the stack cell by pumps during operations. Of the flow battery system, redox flow batteries (RFBs) have been widely demonstrated with various combinations of elements consisting of positive and negative redox couples. In particular, the RFB systems including Fe/Cr [7-9], Zn/Br_2 (ZBB) [10], and polysulfide/Br_2 [11] as well as vanadium RFB (VRFB) [12-14] have been proposed and developed. Of them, VRFB is most famous because it uses the same material in both negative and positive sides of half-cells, which can avoid damage by deep discharge and cross-contamination of the two half-cell electrolytes [14]. Electrolyte solutions of the VRFB consist of sulfuric acid containing vanadium redox couples and the vanadium is divided into four different ionic states: V^{2+}, V^{3+}, VO^{2+} (V^{4+}) and VO_2^+ (V^{5+}). The electrochemical reactions that occur in the electrodes of the VRFB can be expressed as the following equations:

$$\text{At negative side:} \quad V^{2+} \leftrightarrow V^{3+} + e^-, \quad E^o = -0.255 \text{ V vs. SHE} \tag{1}$$

$$\text{At positive side:} \quad VO^{2+} + H_2O \leftrightarrow VO_2^+ + 2H^+ + e^-, \quad E^o = 1.004 \text{ V vs. SHE} \tag{2}$$

Besides vanadium-based electrolytes, ion exchange membrane (IEM) plays a significant role in improving the reliability and performance in the VRFB single cell [15]. Of them, proton exchange membrane (PEM) has been mostly considered for a VRFB as a cell separator and proton conductor for its capability to promote proton transport between negative and positive electrodes and to hinder crossover of vanadium ion [16].

The IEM used in VRFB separates both sides to fend off mixing of electrolytes through the membrane while exchanging proton. However, the undesirable vanadium ion crossover should be minimized because permeation of the vanadium ion decreases VRFB performance with self-discharging and production of mixed potential, resulting in efficiency loss and VRFB cell failure. In addition, the membranes for VRFB are affected by the self-discharging effect and their stability can be worsened. For these reasons, perfluorosulfonic acid proton exchange membranes, such as Nafion® that have high chemical stability and proton conductivity, have been widely used in VRFB systems.

†To whom correspondence should be addressed.
E-mail: kwony@seoultech.ac.kr, sunhoekim@sangji.ac.kr

Vijayakumar et al. [17] analyzed Nafion® membrane in terms of vanadium cation mobilization with analysis by UV-*vis* spectrophotometer (UV vis) and x-ray photoelectron spectroscopy (XPS). Chen et al. [18] optimized membrane thickness with results of charge/discharge curves, efficiencies and polarization curves of the cell. Also, there have been some research results using anion exchange membrane as VRFB separator by Hwang and Ohya [19]. They explained the ease of using anion exchange membrane as a cell separator. Efforts to improve the performance of VRFB by adding inorganic materials, such as silica and TiO_2, to Nafion®, were reported by Teng et al. [20].

Our purpose was to investigate the effect of membrane thickness on performance of VRFB. We compared two different thicknesses of Nafion® membranes, 175 and 50 μm, and evaluated their influence on VRFB performance by measurements of charge and discharge performance, stability, efficiency and vanadium ion permeability. Resistances of vanadium reactions that occurred during operation of VRFB were characterized by electrochemical impedance spectroscopy (EIS) technique. Also, vanadium ion crossover in different thicknesses of membranes was measured by using UV-vis.

EXPERIMENTAL

A VRFB single cell with 25 cm^2 of active area was used in this paper. Two tanks filled with electrolytes for both negative and positive electrodes were installed as reservoirs, while the electrolytes were circulated by pumps. Its approximate schematic including main components is shown in Fig. 1. Two different thicknesses of membranes, Nafion® 117 and Nafion® 212 that have 175 and 50 μm of thickness, respectively, were prepared and their VRFB performance was compared. Carbon felt (PAN graphite felt, XF30A, Toyobo, Japan) with a thickness of 5 mm was used as electrode for both negative and positive electrodes. Electrochemical charge/discharge measurements were done using a computer connected potentiostat (HCP-803, Biologic, USA). Charging and discharging current density were controlled and the related resulting data were collected. The reservoirs put in both negative and positive electrodes were filled with a solution including 1 M $VOSO_4$ and 1 M H_2SO_4. The $VOSO_4$ and

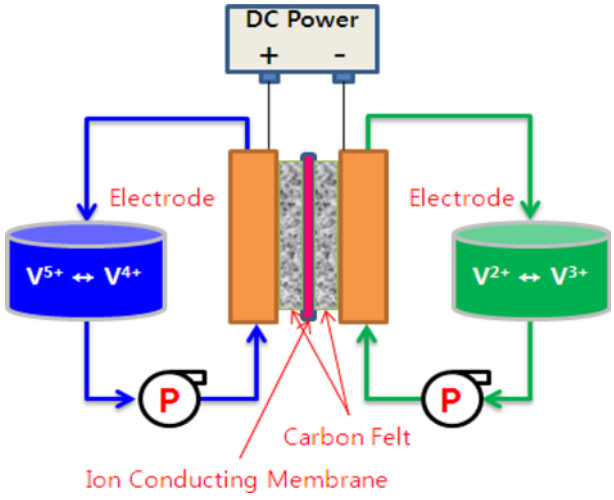

Fig. 1. Schematic diagram of VRFB unit cell and its flow system.

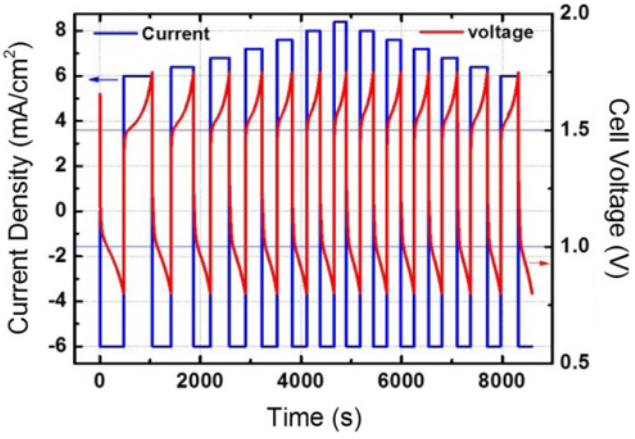

Fig. 2. Typical charge-discharge cycle curves.

H_2SO_4 solutions were mingled in the condition of vigorous stirring until the blue color of vanadium ion appeared. The flow rates of both positive and negative electrolytes were 15 $mLmin^{-1}$.

For this work, the entire VRFB single cell tests were performed by "upward" and "downward" processes. In the "upward" process, as the initial step, a current density of 6.0 mA/cm^2 was applied with the increase in cell voltage until the cell voltage reached charge the cut-off voltage (1.75 V) (the "charging" step), and then the same current density was applied with the decrease in cell voltage until the cell voltage reached discharge cut-off voltage (0.80 V) (the "discharging" step). Once the discharging step was completed, the "charging" and "discharging" steps were repeated with an increase in current density in ascending order (6.0, 6.4, 6.8, 7.2, 7.6, 8.0 and 8.4 mA/cm^2). On the other hand, in the "downward" process, the overall sequence were all the same as the "upward" process except current densities were applied in descending order (8.4, 8.0, 7.6, 7.2, 6.8, 6.4 and 6.0 mA/cm^2). The charge-discharge cycle was repeated continuously ten times. Fig. 2 shows a typical charge-discharge cycle that includes "upward" and "downward" processes.

The EIS of all the samples was performed by using a frequency response analyzer (FRA) combined with potentiostat module. By coupling the FRA with the potentiostat, modulation of direct current was possible. The impedance spectra were taken in the frequency range of 100 kHz to 100 mHz with ten steps per decade. The modulating voltage was 10 mV. A Nyquist plot was used to present the impedance spectra; the diameter of a semicircle in the plot indicates the charge transfer resistance. To attain the value, a Randle's circuit model was adopted [21].

Vanadium ion crossover was estimated using a UV-vis (Optizen 3220UV, Mechasis, Korea) by measuring absorbance of $VOSO_4$ (V^{4+} ion) in all Nafion® membranes. In the UV-vis spectra, the main absorbance peak of the $VOSO_4$ was observed at a wavelength of 750 nm.

More specifically, one reservoir (reservoir 1) was filled with a mixture of 1.0 M $VOSO_4$ and 1.0 M H_2SO_4 solution, while the other reservoir (reservoir 2) was filled with a mixture of 1.0 M $VOSO_4$ and 1.0 M $MgSO_4$. $MgSO_4$ solution was used to minimize osmotic pressure effect and to be on a par with ionic strength of two mixtures [22]. The crossover rates of all Nafion® membranes were measured in the following manner: $VOSO_4$ and $MgSO_4$ solutions were

circulated at the flow rate of 15 $mLmin^{-1}$ at both reservoirs without electric load for the sake of checking out the effect of physical circulation. In actual experiments, VRFB single cells using Nafion® 117 and 212 were run continuously, and $MgSO_4$ solution containing V^{4+} ions of reservoir 2 that permeated from $VOSO_4$ of reservoir 1 was periodically extracted and stored after every predetermine time. UV-vis absorbance peaks of all the solutions were then measured at wavelength of 750 nm and compared with the reference to decide concentration of V^{4+} ions within each solution collected [22-24]. The ratio of the UV-vis absorbance of $MgSO_4$ solution including V^{4+} ions to absorbance of pure $MgSO_4$ solution was considered a reference for the calculation of V^{4+} ion concentration that was the amount of vanadium ion crossover. Once the absorbance data were put together, the vanadium ion crossover rate was measured by using the following equation [25,26].

$$V\frac{dC}{dt} = S\frac{P}{T}[C_i - C] \quad (3)$$

where V is the volume of the solution in both compartments, C_i is an initial concentration of vanadium ion, C is concentration of vanadium ion being contained in the $MgSO_4$ reservoir, which is a function of time, S is the exposed membrane area to the solutions, P is the permeability of vanadium ions and T is the thickness of the membrane used.

RESULTS AND DISCUSSION

It is well known that capacity is affected by charging current density. Therefore, it is important to investigate the correlation between the capacity and the charging current density. For doing that, the

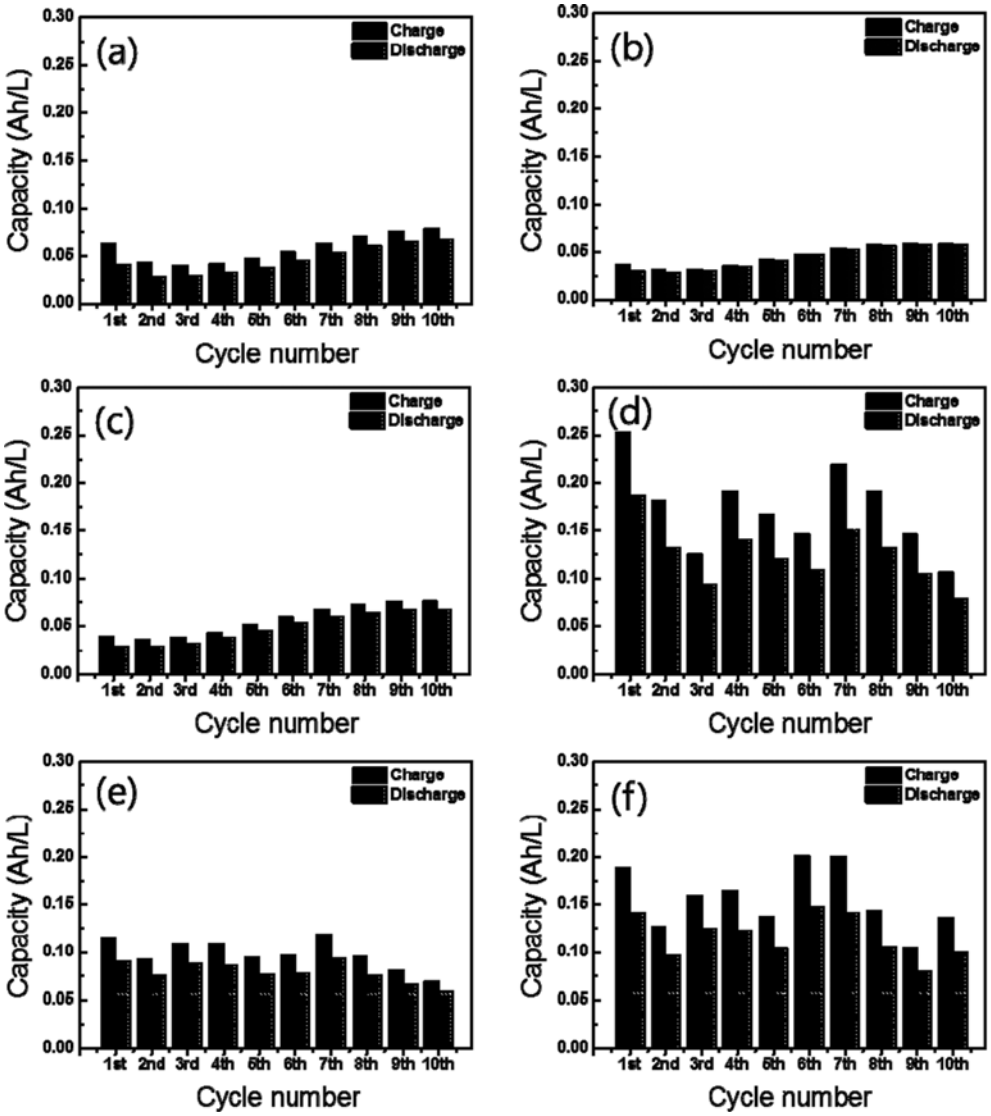

Fig. 3. Changes in amount of charge and discharge with increase in cycle number in different charging current densities; (a) when charging current density is 6.0 mA/cm² with upward process in VRFB single cell using Nafion® 117, (b) when charging current density is 8.4 mA/cm² in VRFB single cell using Nafion® 117, (c) when charging current density is 6.0 mA/cm² with downward process in VRFB single cell using Nafion® 117, (d) when charging current density is 6.0 mA/cm² with upward process in VRFB single cell using Nafion® 212, (e) when charging current density is 8.4 mA/cm² in VRFB single cell using Nafion® 212 and (f) when charging current density is 6.0 mA/cm² with downward process in VRFB single cell using Nafion® 212.

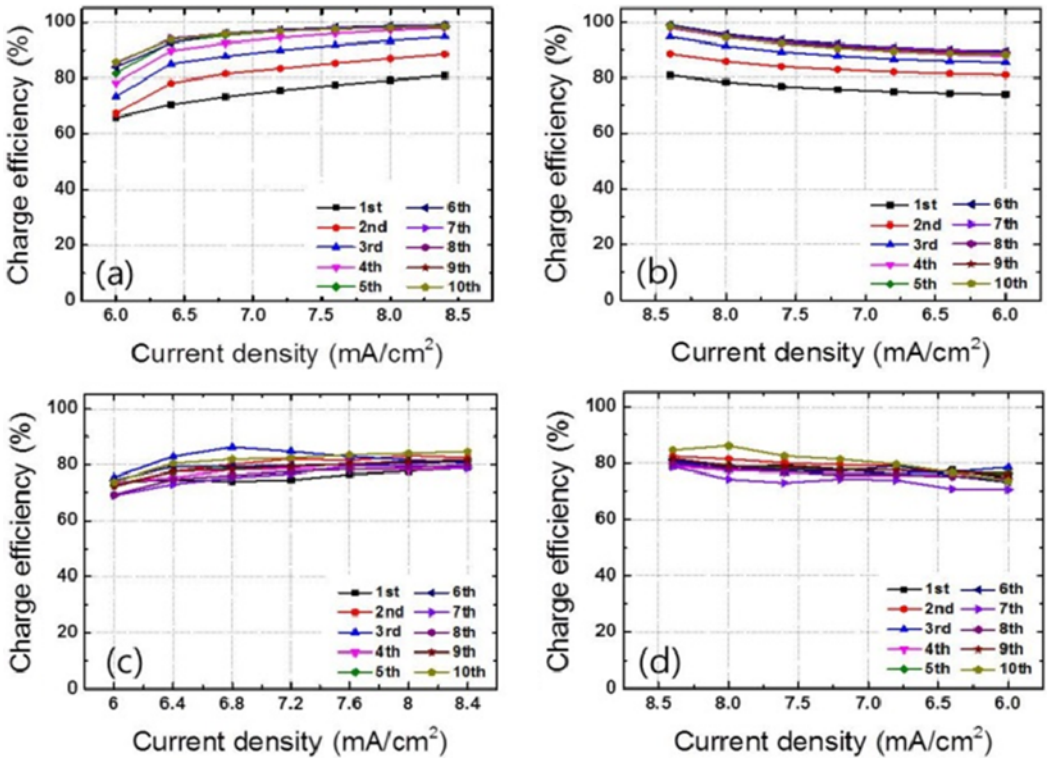

Fig. 4. Charge efficiencies in different charging current densities and membrane thicknesses. (a) upward process of VRFB single cell using Nafion® 117, (b) upward process of VRFB single cell using Nafion® 212, (c) downward process of VRFB single cell using Nafion® 117 and (d) downward process of VRFB single cell using Nafion® 212.

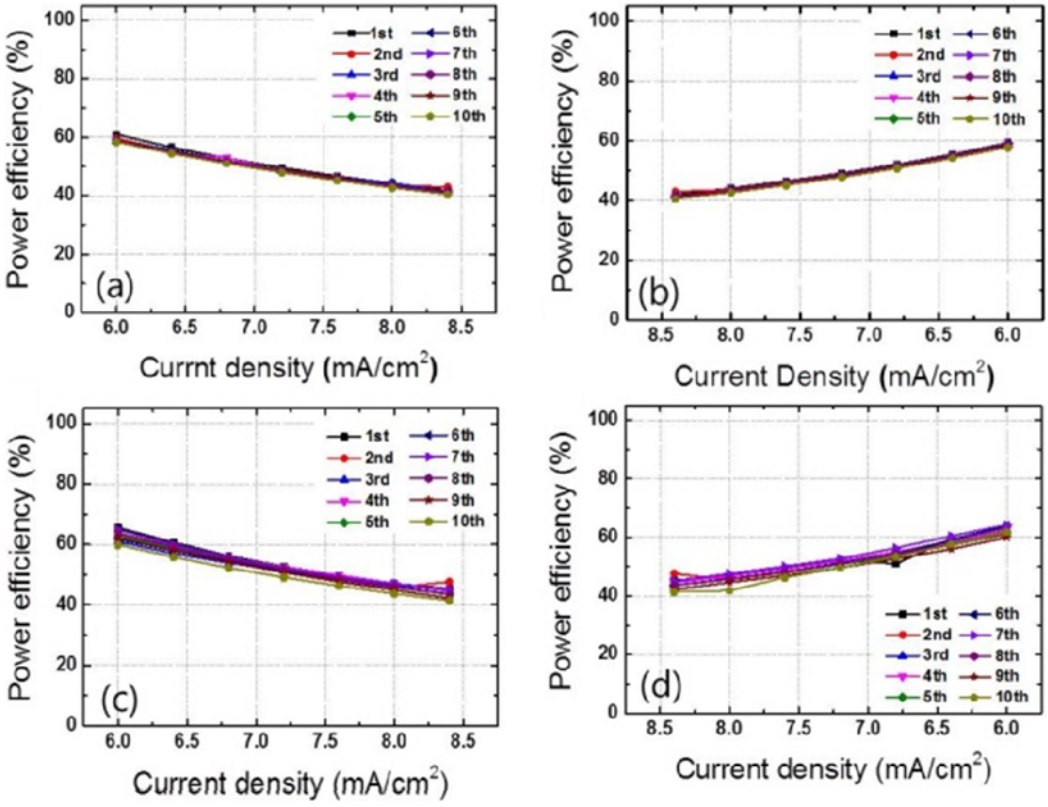

Fig. 5. Power efficiencies in different charging current densities and membrane thicknesses. (a) upward process of VRFB single cell using Nafion® 117, (b) upward process of VRFB single cell using Nafion® 212, (c) downward process of VRFB single cell using Nafion® 117 and (d) downward process of VRFB single cell using Nafion® 212.

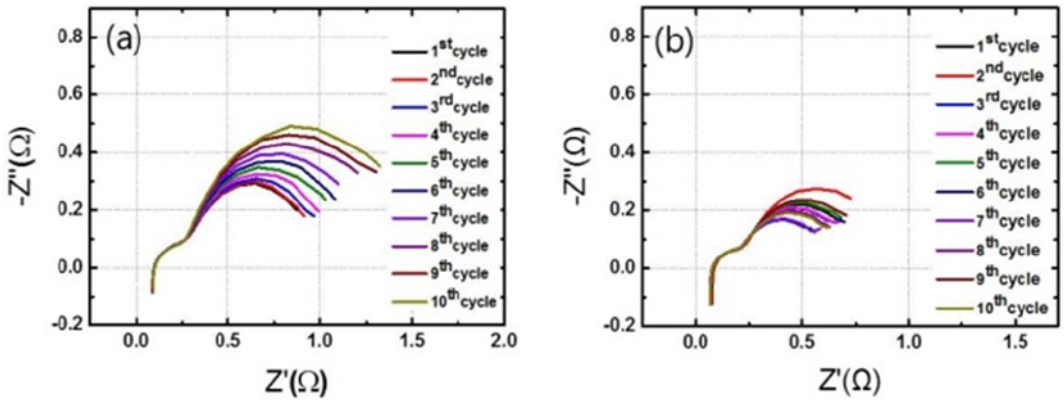

Fig. 6. Nyquist plots of VRFB single cells using (a) Nafion® 117 and (b) Nafion® 212.

"upward" and "downward" charging process was conducted ten times. Fig. 2 shows the first charge-discharge cycle performed at the VRFB single cell using Nafion® 117. According to results gained by the charge-discharge cycle tests, as charging current density increased, charging and discharging times were getting shorter, meaning that the charging and discharging times were reciprocal to charging current density.

To evaluate the effect of membrane thickness on charge and discharge capacities in different charging current densities, the capacities were measured and the result is shown in Fig. 3. Fig. 3(a), (b) and (c) indicate charge and discharge capacities that were measured in VRFB using Nafion® 117 under three different current densities, 6.0 (upward), 8.4 (peak) and 6.0 (downward) mA/cm^2, while Fig. 3(d), (e) and (f) represent the values measured in VRFB using Nafion® 212 instead of Nafion® 117. There are three notable things in the result of Fig. 3: (i) charge and discharge capacities measured in VRFB using Nafion® 212 were more than those measured in VRFB using Nafion® 117, (ii) discharge capacity was less than charge capacity, and (iii) charge capacity was affected by charging current density. As will be explained later, (i) and (ii) were attributed to crossover rate of vanadium ion and charge transfer resistance by electrochemical reaction, and (iii) was ascribed to the change in concentration gradient at double layer, meaning with increase in charging current density, both concentration gradient and overpotential increased. The higher overpotential was, the sooner cell voltage reached charge cut-off voltage and the less the amount of charge was [27].

Fig. 4 shows the charge efficiencies (CEs) of VRFBs using Nafion® 117 and 212. Fig. 4(a) and (b) represent the CEs obtained by VRFB single cell using Nafion® 117, while Fig. 4(c) and (d) represent the CEs obtained by VRFB single cell using Nafion® 212. In the result, CE of the VRFB single cell using Nafion® 117 was better than that of the VRFB single cell using Nafion® 212. The difference in CE is attributed to the difference in crossover rate of vanadium ions in different membrane thicknesses. Because the crossover of vanadium ions is mainly caused by diffusion, the vanadium crossover rate is reciprocal to membrane thickness, meaning that thinner thickness leads to higher concentration gradient, followed by higher vanadium crossover rate [18].

The power efficiencies (PEs) of VRFB single cells using Nafion® 117 and 212 are shown in Fig. 5. Fig. 5(a) and (b) represent the PEs obtained by VRFB single cell using Nafion® 117, while Fig. 5(c) and (d) represent the PEs obtained by VRFB single cell using Nafion® 212. According to the measurements, the PE of VRFB single cells using Nafion® 212 was better than that of VRFB single cells using Nafion® 117. This result is ascribed to electrochemical reaction resistance, which decreases in thinner membrane. Because PE is strongly affected by ohmic loss created from overpotential taking place by Ohm's law, increase in membrane thickness leads to higher reaction resistance by Ohm's law [18,28].

The effect of membrane thickness on CE and PE was further analyzed by using EIS. Fig. 6(a) and (b) are the Nyquist plots of VRFB single cells using Nafion® 117 and 212. In the plots, the diameters of semi-circles represent electrochemical reaction resistances [29]. According to the Nyquist plots, the diameters of semi-circles drawn by Nafion® 117 were larger than those drawn by Nafion® 212. When the EIS data of Fig. 6 was compared to the PE trend of Fig. 5, the two results were well matched, demonstrating that the lower reaction resistance (charge transfer resistance) led to higher PE. One thing to note here is the size of the semicircle diameter of the Nyquist plots. The diameter of the semicircle drawn by Nafion® 117 increases as cycle number increases, while that drawn by Nafion® 212 remains unchanged irrespective of cycle number. This result is probably ascribed to the difference in vanadium ion crossover rate between Nafion® 117 and 212. The vanadium ion crossover is advanced during repetitive charging and discharging processes, result-

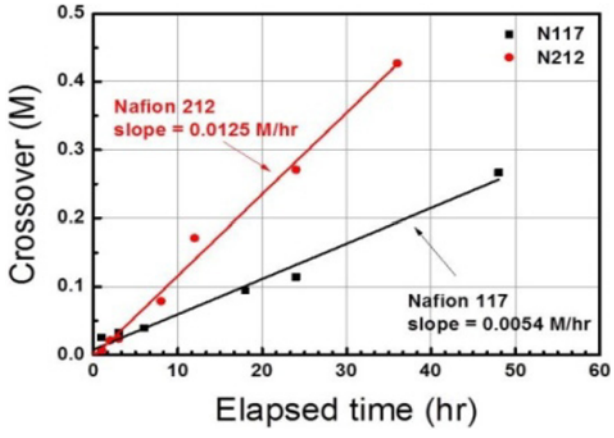

Fig. 7. Vanadium ion crossover rate quantified by UV vis.

ing in repetitive forward and backward migrations by osmotic drag. Although further evaluating is needed, it is believed that with high crossover rate (here, the semicircle drawn by Nafion® 212), the vanadium ion crossover may disturb electrochemical reactions more easily, which causes the irregular size of semicircle diameters.

For evaluation of the effect of vanadium ion crossover on the performance of VRFB single cells, the vanadium ion crossover rate was quantified with UV-vis and the result is summarized in Fig. 7. In the UV-vis spectra, the main absorption peak of vanadium ion (V^{4+} ion) was observed at the wavelength of 750 nm [30]. The changes in concentration of vanadium ions calculated were linearly proportional to operation time. Crossover rate of each sample was determined from the slope of the linear lines that were analyzed by linear regression method. As a result of the calculation, the crossover rate of Nafion® 212 (0.0125 M/hr) was higher than that of Nafion® 117 (0.0054 M/hr). This result makes sense because crossover is expected to be more active in thinner membrane, and this trend was well matched with CE data of Fig. 4.

The energy efficiencies (EEs) of VRFB single cells using Nafion® 117 and 212 are shown in Fig. 8. Fig. 8(a) and (b) represent the EEs obtained by VRFB single cell using Nafion® 117, while Fig. 8(c) and (d) show the EEs obtained by VRFB single cell using Nafion® 212. In the Fig. 8, EE of VRFB single cell using Nafion® 117 is better than that of VRFB single cell using Nafion® 212. Because EE is a product of CE and PE, Fig. 8 means that crossover of vanadium ions has a more important role than electrochemical reaction resistance in determining the performance of VRFB single cells using Nafion membranes. This result also explains well the general attribute of the Nafion membrane that has high crossover rate (high permeability) of fuels [31].

The performance of VRFB single cells with two different membrane thicknesses was estimated and the effect of membrane thickness on the performance of VRFB single cell was compared. When it came to the amount of charge and discharge measured in different charging current densities, the amount of VRFB using Nafion® 212 was more than that of VRFB using Nafion® 117. Also, when the efficiencies of VRFB single cells were measured, CE and EE of VRFB using Nafion® 117 were higher than those of VRFB using Nafion® 212, whereas PE showed the opposite result.

CONCLUSION

Such results were due to both vanadium crossover rate and electrochemical reaction resistance based on Ohm's law. Namely, as membrane thickness decreased, the vanadium crossover rate increased and CE decreased because the CE relied on the vanadium crossover rate. The result explains CE of VRFB using thick Nafion® 117 is superior to that using thin Nafion® 117. In contrast, the electrochemical reaction resistance decreased with an increase in membrane thickness due to Ohm's law and the correlation between resistance and resistivity, and thus, PE affected by the reaction resistance decreased. The result explains that PE of VRFB using thin Nafion® 117 is superior to that using thick Nafion® 212.

Because EE of VRFB using Nafion® 117 was higher than that

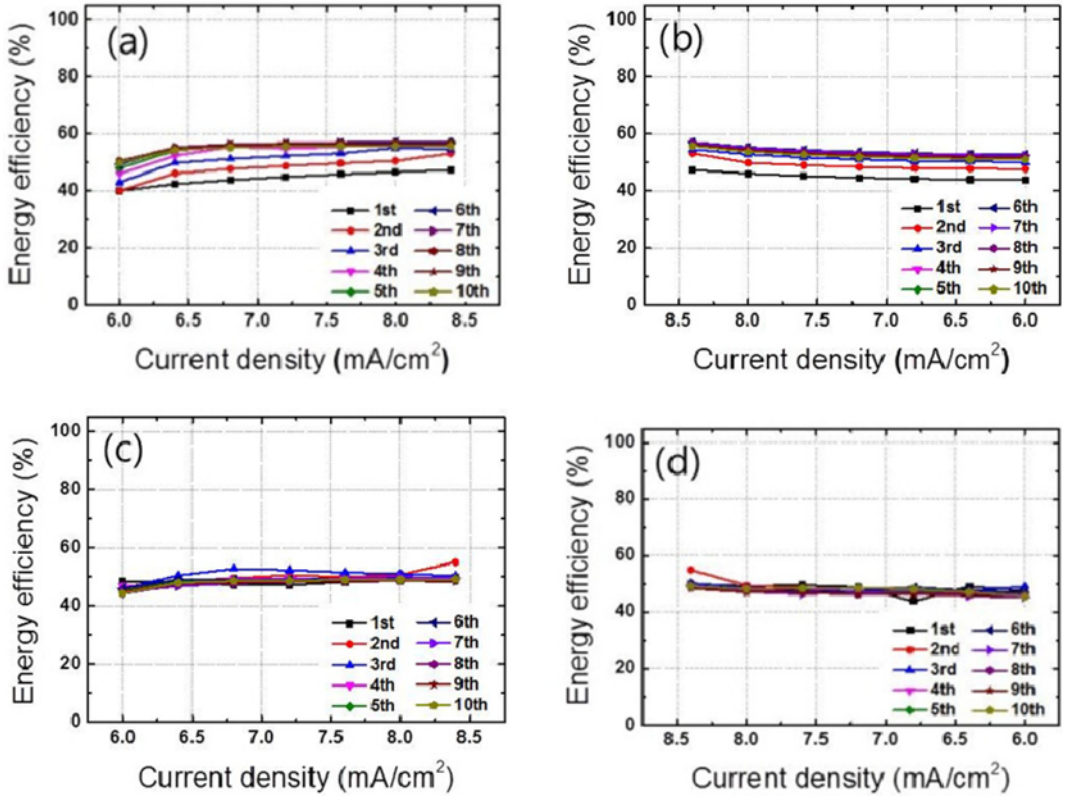

Fig. 8. Energy efficiencies in different charging current densities and membrane thicknesses. (a) upward process of VRFB single cell using Nafion® 117, (b) upward process of VRFB single cell using Nafion® 212, (c) downward process of VRFB single cell using Nafion® 117 and (d) downward process of VRFB single cell using Nafion® 212.

of VRFB using Nafion® 212, it is reasonable to say that crossover of vanadium ions had a more important role than electrochemical reaction resistance in deciding the performance of VRFB when Nafion membranes were used.

To further inspect the effect of membrane thickness on VRFB performance, EIS and UV-vis measurements were performed. According to the EIS, due to high crossover rate of vanadium ions in VRFB using Nafion® 212, EIS result of VRFB using Nafion® 117 was more stable. The vanadium ion crossover rate of Nafion® 117 and 212 quantified by the UV-vis was 0.0054 M/hr and 0.0125 M/hr, respectively. These characterization results are well matched with the performance data of VRFB single cell.

ACKNOWLEDGEMENTS

This research was supported by the Sangji University Research Fund 2012 and by 2014 Human Resource Cultivation Program for Graduate School of Environment and Energy of Sudokwon Landfill Site Management.

REFERENCES

1. R. Landgrebe and S. W. Donley, *Appl. Energy*, **15**, 127 (1983).
2. M. Skyllas-Kazacos, M. Rychcik, R. Robins, A. G. Fane and M. A. Green, *J. Electrochem. Soc.*, **133**, 1057 (1986).
3. Z. G. Yang, J. L. Zhang and M. C. Kintner, *Chem. Rev.*, **111**, 3577 (2011).
4. E. Sum, M. Rychcik and M. Skyllas-Kazacos, *J. Power Sources*, **16**, 85 (1985).
5. C. P. De Leon, A. F. Ferrer, J. G. Garcia, D. A. Szanto and F. C. Walsh, *J. Power Sources*, **160**, 716 (2006).
6. K. L. Huang, X. G. Li, S. Q. Liu, N. Tan and L. Q. Chen, *Renew Energy*, **33**, 186 (2008).
7. L. H. Thaller, *NASA TM-X-71540*, 168 (1974).
8. T. Yamamura, Y. Shiokawa, H. Yamana and H. Moriyama, *Electrochim. Acta*, **48**, 43 (2002).
9. B. Fang, S. Iwasa, Y. Wei, T. Arai and M. Kumagai, *Electrochim. Acta*, **47**, 3971 (2002).
10. P. C. Butler, P. A. Eidler, P. G. Grimes, S. E. Klassen and R. C. Miles, *Zinc/Bromine Batteries, in Handbook of Batteries (Ed.: David Linden, Thomas B. Reddy)*, McGraw-Hill, Ohio (2001).
11. H. T. Zhou, H. M. Zhang, P. Zhao and B. L. Yi, *Electrochim. Acta*, **51**, 6304 (2006).
12. W. Wang, H. Zhang, X. Li, Z. Mai and H. Zhang, *J. Power Sources*, **208**, 421 (2012).
13. M. Skyllas-Kazacos, M. Rychcik, R. G. Robins, A. G. Fane and M. A. Green, *J. Electrochem. Soc.*, **133**, 1057 (1986).
14. S. Chung, S. Kim and Y. Kwon, *Electrochim. Acta*, **114**, 439 (2013).
15. M. Skyllas-Kazacos, G. Kazacos, G. Poon and H. Verseema, *Int. J. Energy Res.*, **34**, 174 (2010).
16. T. Sukkar and M. Skyllas-Kazacos, *J. Membr. Sci.*, **222**, 249 (2003).
17. M. Vijayakumar, M. S. Bhuvaneswari, P. Nachimuthu, B. Schwenzer, S. Kim, Z. Yang, J. Liu, G. L. Graff, S. Thevuthasan and J. Hu, *J. Membr. Sci.*, **366**(1-2), 325 (2011).
18. D. Chen, M. A. Hickner, E. Agar and E. C. Kumbur, *J. Membr. Sci.*, **437**, 108 (2013).
19. G. Hwang and H. Ohya, *J. Membr. Sci*., **132**, 55 (1997).
20. X. Teng, Y. Zhao, J. Xi, Z. Wu, X. Qiu and L. Chen, *J. Membr. Sci.*, **341**(1-2), 149 (2009).
21. S. M. Baik, J. Kim, J. Han and Y. Kwon, *Int. J. Hydrogen Energy*, **36**, 14719 (2011).
22. Q. Luo, H. Zhang, J. Chen, P. Qian and Y. Zhai, *J. Membr. Sci.*, **311**, 98 (2008).
23. T. Mohammadi and M. Skyllas-Kazacos, *J. Power Sources*, **63**, 179 (1996).
24. T. Mohammadi and M. Skyllas-Kazacos, *J. Appl. Electrochem.*, **27**, 153 (1997).
25. M. S. Kang, Y. J. Choi and S. H. Moon, *J. Membr. Sci.*, **207**, 157 (2002).
26. X. Luo, Z. Lu, J. Xi, Z. Wu, W. Zhu, L. Chen and X. Qiu, *J. Phys. Chem. B*, **109**, 20310 (2005).
27. J. Marcicki, A. Conlisk and G. Rizzoni, *J. Power Sources*, **251**, 157 (2014).
28. D. Chen, M. A. Hickner, E. Agar and E. C. Kumbur, *Electrochem. Commun.*, **26**, 37 (2013).
29. S. M. Baik, J. Kim, J. Han and Y. Kwon, *Int. J. Hydrogen Energy*, **36**, 12583 (2011).
30. N. H. Choi, S. K. Kwon and H. Kim, *J. Electrochem. Soc.*, **160**, A973 (2013).
31. V. Neburchilov, J. Martin, H. Wangand J. Zhang, *J. Power Sources*, **169**, 221 (2007).